Ab Initio Calculations of Nuclear Structure (and Reactions)

Goals

Understand nuclei at the level of elementary interactions between individual nucleons, including

- Binding energies, excitation spectra, relative stability
- Densities, electromagnetic moments, transition amplitudes, cluster-cluster overlaps
- Low-energy NA & AA scattering, astrophysical reactions

Requirements

- Two-nucleon potentials that accurately describe elastic NN scattering data
- Consistent many-nucleon potentials and electroweak current operators
- Precise methods for solving the many-nucleon Schrödinger equation

Issues to Discuss

- Theoretical advantages and limitations of a given Hamiltonian or method
- What benchmarks to calculate for comparison of different methods
- What experiments to test and refine our models and methods

Recent Developments in Nuclear Quantum Monte Carlo

Robert B. Wiringa
Physics Division, Argonne National Laboratory

Work with

Joe Carlson, Los Alamos

Laura Marcucci, Pisa

Ken Nollett, Argonne

Muslema Pervin, Argonne

Steve Pieper, Argonne

Rocco Schiavilla, JLab & ODU

Work not possible without extensive computer resources

Argonne LCRC (Jazz), MCS Division (BlueGene/L), and ALCF (BlueGene/P)

NERSC IBM SP's (Seaborg, Bassi)

UNEDF SciDAC and INCITE programs

Argonne NATIONAL LABORATORY

Physics Division

Work supported by U.S. Department of Energy, Office of Nuclear Physics

Outline

Hamiltonian

Variational Monte Carlo

Green's function Monte Carlo

Binding energy results

Nolen-Schiffer anomaly & ^{8}Be isospin-mixing

Densities and radii

Meson-exchange currents and magnetic moments

$M1$, $E2$, F, GT transitions

NA scattering & astrophysical reactions

Nucleon momentum distributions & $A(e,e'pN)$

HAMILTONIAN

$$H = \sum_i K_i + \sum_{i<j} v_{ij} + \sum_{i<j<k} V_{ijk}$$

$$K_i = K_i^{CI} + K_i^{CSB} \equiv -\frac{\hbar^2}{4}[(\frac{1}{m_p} + \frac{1}{m_n}) + (\frac{1}{m_p} - \frac{1}{m_n})\tau_{zi}]\nabla_i^2$$

Argonne v_{18} (AV18)

$$v_{ij} = v_{ij}^{\gamma} + v_{ij}^{\pi} + v_{ij}^{I} + v_{ij}^{S} = \sum_p v_p(r_{ij})O_{ij}^p$$

v_{ij}^{γ}: pp, pn & nn electromagnetic terms

$$v_{ij}^{\pi} \sim [Y_\pi(r_{ij})\sigma_i \cdot \sigma_j + T_\pi(r_{ij})S_{ij}] \otimes \tau_i \cdot \tau_j$$

$$v_{ij}^{I} = \sum_p I^p T_\pi^2(r_{ij})O_{ij}^p$$

$$v_{ij}^{S} = \sum_p [P^p + Q^p r + R^p r^2]W(r)O_{ij}^p$$

$$\begin{aligned} O_{ij}^p = & [1, \sigma_i \cdot \sigma_j, S_{ij}, \mathbf{L}\cdot\mathbf{S}, \mathbf{L}^2, \mathbf{L}^2(\sigma_i \cdot \sigma_j), (\mathbf{L}\cdot\mathbf{S})^2] \\ & + [1, \sigma_i \cdot \sigma_j, S_{ij}, \mathbf{L}\cdot\mathbf{S}, \mathbf{L}^2, \mathbf{L}^2(\sigma_i \cdot \sigma_j), (\mathbf{L}\cdot\mathbf{S})^2] \otimes \tau_i \cdot \tau_j \\ & + [1, \sigma_i \cdot \sigma_j, S_{ij}, \mathbf{L}\cdot\mathbf{S}] \otimes T_{ij} \\ & + [1, \sigma_i \cdot \sigma_j, S_{ij}, \mathbf{L}\cdot\mathbf{S}] \otimes (\tau_i + \tau_j)_z \end{aligned}$$

$$S_{ij} = 3\sigma_i \cdot \hat{r}_{ij}\sigma_j \cdot \hat{r}_{ij} - \sigma_i \cdot \sigma_j \qquad T_{ij} = 3\tau_{iz}\tau_{jz} - \tau_i \cdot \tau_j$$

Argonne v_{18}

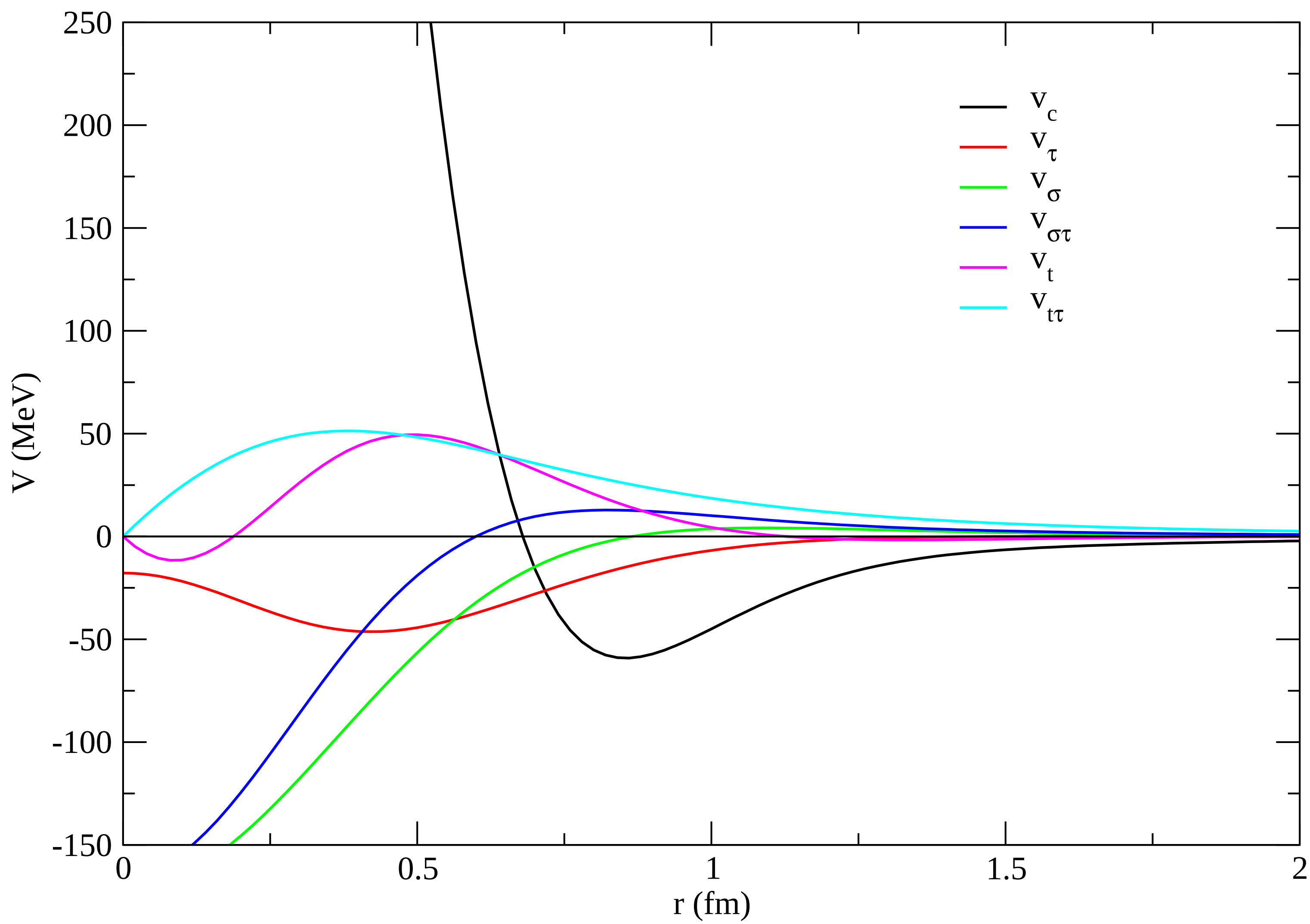

Fits Nijmegen PWA93 data base of 1787 pp & 2514 np observables for $E_{lab} \leq 350$ MeV with χ^2/datum = 1.1 plus nn scattering length and ^{2}H binding energy

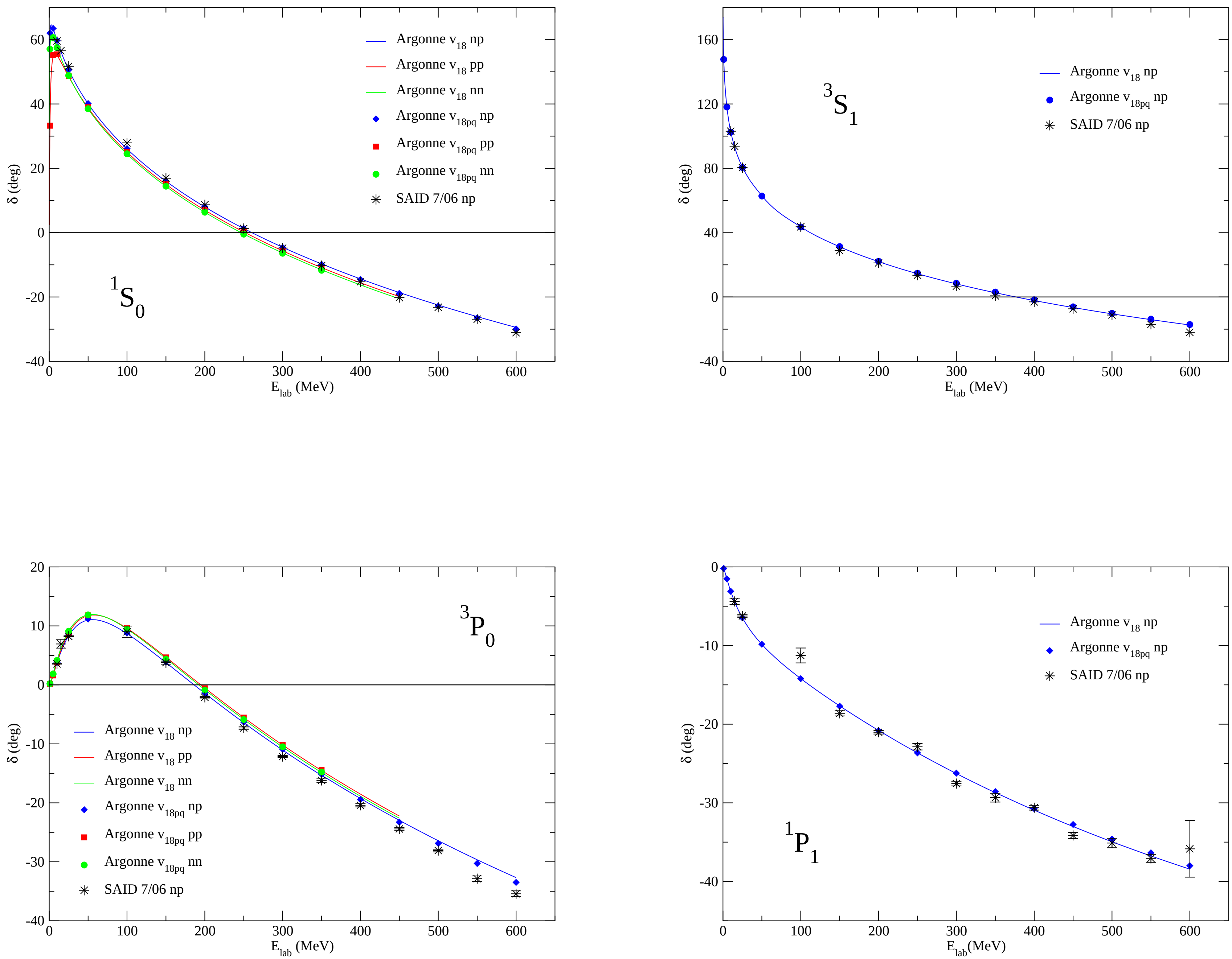

$^1S_0$
$^3S_1$
$^3P_0$
$^1P_1$
δ (deg)
E_{lab} (MeV)
Argonne v_{18} np
Argonne v_{18} pp
Argonne v_{18} nn
Argonne v_{18pq} np
Argonne v_{18pq} pp
Argonne v_{18pq} nn
SAID 7/06 np

Three-nucleon potentials

Urbana (UIX)

$$V_{ijk} = V_{ijk}^{2\pi P} + V_{ijk}^{R}$$

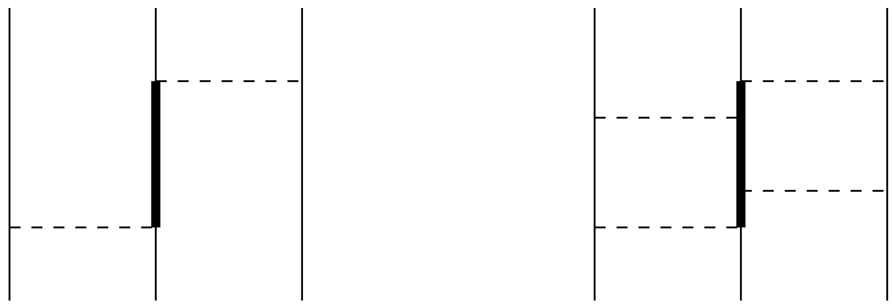

Illinois (IL2,IL7)

$$V_{ijk} = V_{ijk}^{2\pi P} + V_{ijk}^{2\pi S} + V_{ijk}^{3\pi\Delta R} + V_{ijk}^{R} + V_{ijk}^{R\tau}$$

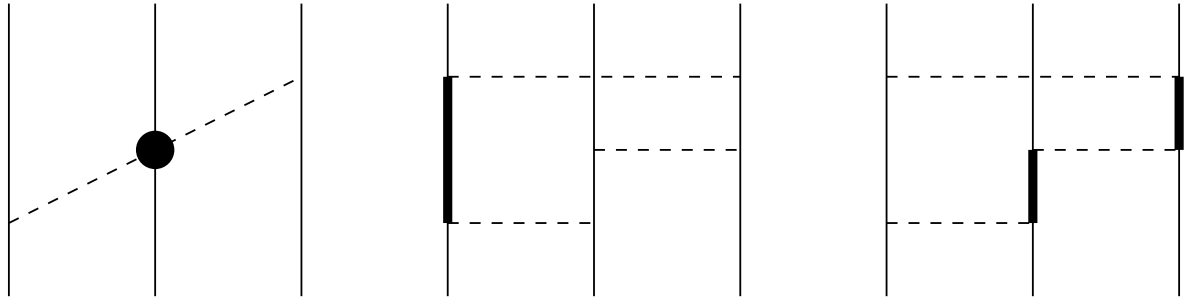

Variational Monte Carlo

Minimize expectation value of H

$$E_V = \frac{\langle \Psi_V | H | \Psi_V \rangle}{\langle \Psi_V | \Psi_V \rangle} \geq E_0$$

Trial function (s-shell nuclei)

$$|\Psi_V\rangle = \left[1 + \sum_{i<j<k} U_{ijk}^{TNI} \right] \left[\mathcal{S} \prod_{i<j} (1 + U_{ij}) \right] |\Psi_J\rangle$$

$$|\Psi_J\rangle = \left[\prod_{i<j} f_c(r_{ij}) \right] |\Phi_A(JMTT_3)\rangle$$

$$|\Phi_d(1100)\rangle = \mathcal{A} | \uparrow p \uparrow n \rangle \;\; ; \;\; |\Phi_\alpha(0000)\rangle = \mathcal{A} | \uparrow p \downarrow p \uparrow n \downarrow n \rangle$$

$$U_{ij} = \sum_{p=2,6} u_p(r_{ij}) O_{ij}^p \;\; ; \;\; U_{ijk}^{TNI} = -\epsilon V_{ijk}(\tilde{r}_{ij}, \tilde{r}_{jk}, \tilde{r}_{ki})$$

Functions $f_c(r_{ij})$ and $u_p(r_{ij})$ obtained from coupled differential equations with v_{ij} .

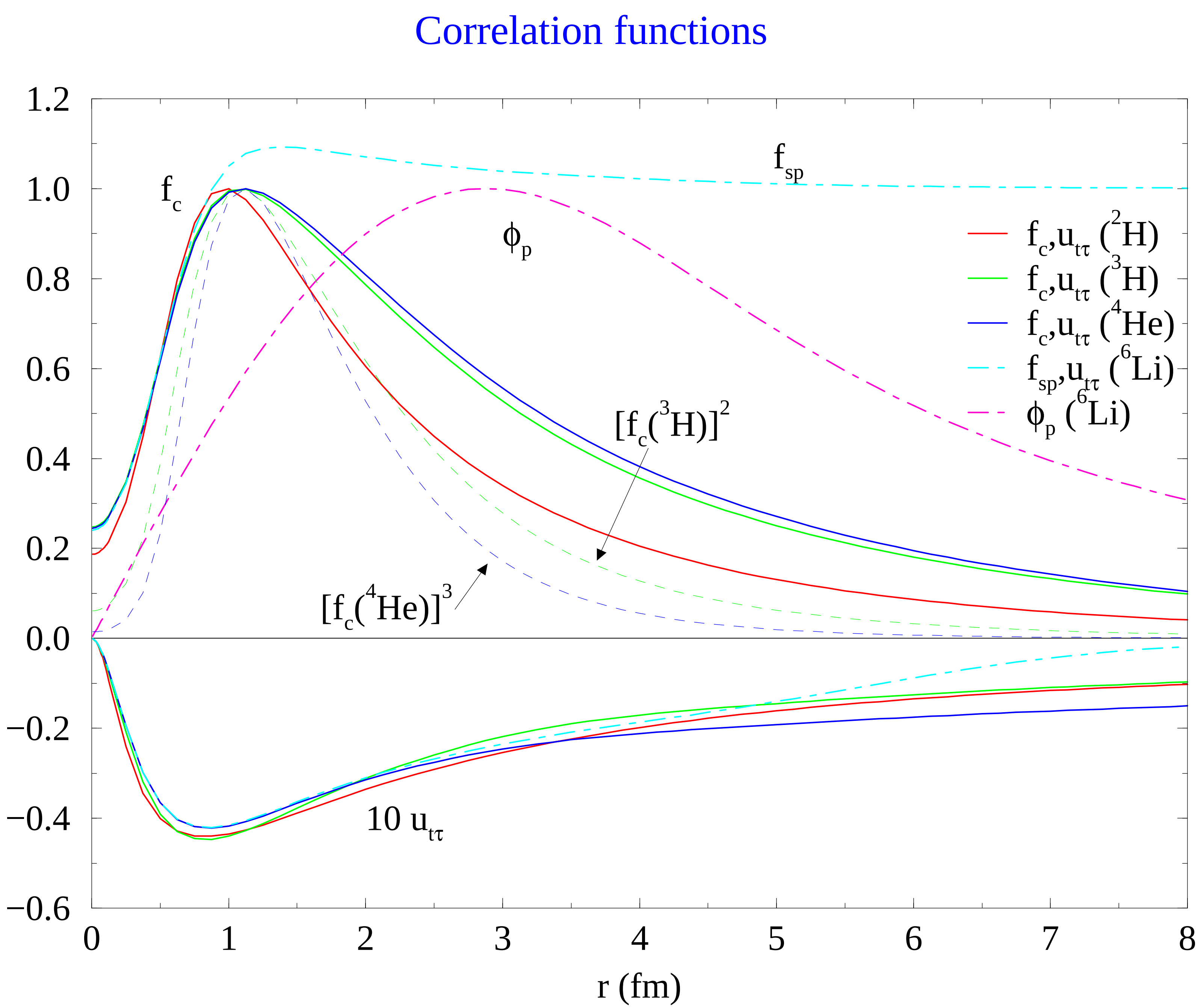

Correlation functions
1.2
1.0
0.8
0.6
0.4
0.2
0.0
−0.2
−0.4
−0.6
0
1
2
3
4
5
6
7
8
r (fm)
f_c
f_{sp}
ϕ_p
$[f_c(^3H)]^2$
$[f_c(^4He)]^3$
$10\ u_{t\tau}$
$f_c, u_{t\tau}$ (^{2}H)
$f_c, u_{t\tau}$ (^{3}H)
$f_c, u_{t\tau}$ (^{4}He)
$f_{sp}, u_{t\tau}$ (^{6}Li)
ϕ_p (^{6}Li)

Trial function (p-shell nuclei)

$$|\Psi_J\rangle = \mathcal{A}\left\{ \prod_{i<j\leq 4} f_{ss}(r_{ij}) \sum_{LS[n]} \beta_{LS[n]} \prod_{k\leq 4<l\leq A} f_{sp}(r_{kl}) \prod_{4<l<m\leq A} f_{pp}(r_{lm}) \right.$$

$$\left. \left| \Phi_\alpha(0000)_{1234} \prod_{4<l\leq A} \phi_p^{LS[n]}(R_{\alpha l}) \left\{ [Y_1^{m_l}(\Omega_{\alpha l})]_{LM_L} \otimes [\chi_l(\tfrac{1}{2}m_s)]_{SM_S} \right\}_{JM} [\nu_l(\tfrac{1}{2}t_3)]_{TT_3} \right\rangle \right\}$$

Diagonalization

in $\beta_{LS[n]}$ basis to produce energy spectra $E(J^\pi_x)$ and orthogonal excited states $\Psi_V(J^\pi_x)$

Expectation values

$\Psi_V(\mathbf{R})$ represented by vector with $2^A \times \binom{A}{Z}$ spin-isospin components for each space configuration $\mathbf{R} = (\mathbf{r}_1, \mathbf{r}_2, ..., \mathbf{r}_A)$; Expectation values are given by summation over samples drawn from probability distribution $W(\mathbf{R}) = |\Psi_P(\mathbf{R})|^2$:

$$\frac{\langle\Psi_V|O|\Psi_V\rangle}{\langle\Psi_V|\Psi_V\rangle} = \sum \frac{\Psi_V^\dagger(\mathbf{R})O\Psi_V(\mathbf{R})}{W(\mathbf{R})} \Big/ \sum \frac{\Psi_V^\dagger(\mathbf{R})\Psi_V(\mathbf{R})}{W(\mathbf{R})}$$

$\Psi^\dagger\Psi$ is a dot product and $\Psi^\dagger O\Psi$ a sparse matrix operation.

Green's Function Monte Carlo

Projects out lowest energy state from variational trial function

$$\Psi(\tau) = \exp[-(H - E_0)\tau]\Psi_V = \sum_n \exp[-(E_n - E_0)\tau] a_n \psi_n$$
$$\Psi(\tau \to \infty) = a_0 \psi_0$$

Evaluation of $\Psi(\tau)$ done stochastically in small time steps $\Delta\tau$

$$\Psi(\mathbf{R}_n, \tau) = \int G(\mathbf{R}_n, \mathbf{R}_{n-1}) \cdots G(\mathbf{R}_1, \mathbf{R}_0) \Psi_V(\mathbf{R}_0) d\mathbf{R}_{n-1} \cdots d\mathbf{R}_0$$

using the short-time propagator accurate to order $(\Delta\tau)^3$ (V_{ijk} term omitted for simplicity)

$$G_{\alpha\beta}(\mathbf{R}, \mathbf{R}') = e^{E_0 \delta\tau} G_0(\mathbf{R}, \mathbf{R}') \langle\alpha| \left[\mathcal{S} \prod_{i<j} \frac{g_{ij}(\mathbf{r}_{ij}, \mathbf{r}'_{ij})}{g_{0,ij}(\mathbf{r}_{ij}, \mathbf{r}'_{ij})} \right] |\beta\rangle$$

where the free many-body propagator is

$$G_0(\mathbf{R}, \mathbf{R}') = \langle \mathbf{R} | e^{-K \triangle\tau} | \mathbf{R}' \rangle = \left[\sqrt{\frac{m}{2\pi\hbar^2 \triangle\tau}} \right]^{3A} \exp\left[\frac{-(\mathbf{R} - \mathbf{R}')^2}{2\hbar^2 \triangle\tau / m} \right]$$

and $g_{0,ij}$ and g_{ij} are the free and exact two-body propagators

$$g_{ij}(\mathbf{r}_{ij}, \mathbf{r}'_{ij}) = \langle \mathbf{r}_{ij} | e^{-H_{ij} \triangle\tau} | \mathbf{r}'_{ij} \rangle$$

Mixed estimates

$$\langle O(\tau)\rangle = \frac{\langle\Psi(\tau)|O|\Psi(\tau)\rangle}{\langle\Psi(\tau)|\Psi(\tau)\rangle} \approx \langle O(\tau)\rangle_{\rm Mixed} + [\langle O(\tau)\rangle_{\rm Mixed} - \langle O\rangle_V]$$

$$\langle O(\tau)\rangle_{\rm Mixed} = \frac{\langle\Psi_V|O|\Psi(\tau)\rangle}{\langle\Psi_V|\Psi(\tau)\rangle} \quad ; \quad \langle H(\tau)\rangle_{\rm Mixed} = \frac{\langle\Psi(\tau/2)|H|\Psi(\tau/2)\rangle}{\langle\Psi(\tau/2)|\Psi(\tau/2)\rangle} \geq E_0$$

Propagator cannot contain spin or isospin-dependent p^2, L^2, or $(\mathbf{L}\cdot\mathbf{S})^2$ operators:

$G_{\beta\alpha}(\mathbf{R}',\mathbf{R})$ has only v_8'

$\langle v_{18} - v_8'\rangle$ computed perturbatively with extrapolation (small for AV18)

Fermion sign problem limits maximum τ:

$G_{\beta\alpha}(\mathbf{R}',\mathbf{R})$ brings in lower-energy boson solution

$\langle\Psi_V|H|\Psi(\tau)\rangle$ projects back fermion solution. but statistical errors grow exponentially

Constrained-path propagation, removes steps that have

$$\overline{\Psi^\dagger(\tau,\mathbf{R})\Psi(\mathbf{R})} = 0$$

Possible systematic errors rduced by $10-20$ unconstrained steps before evaluating observables.

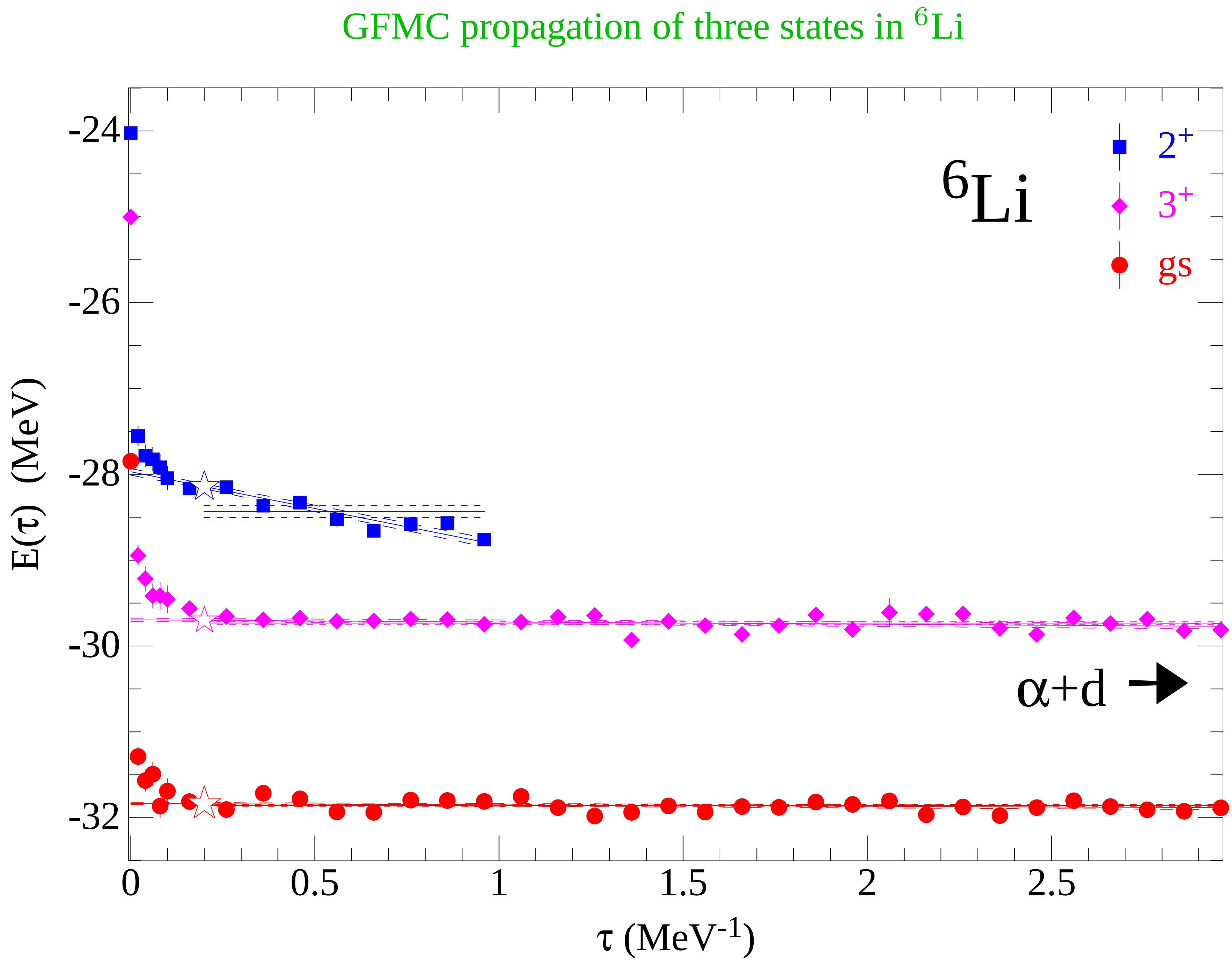
GFMC propagation of three states in 6Li
6Li
2+
3+
gs
α+d
E(τ) (MeV)
τ (MeV-1)
-24
-26
-28
-30
-32
0
0.5
1
1.5
2
2.5

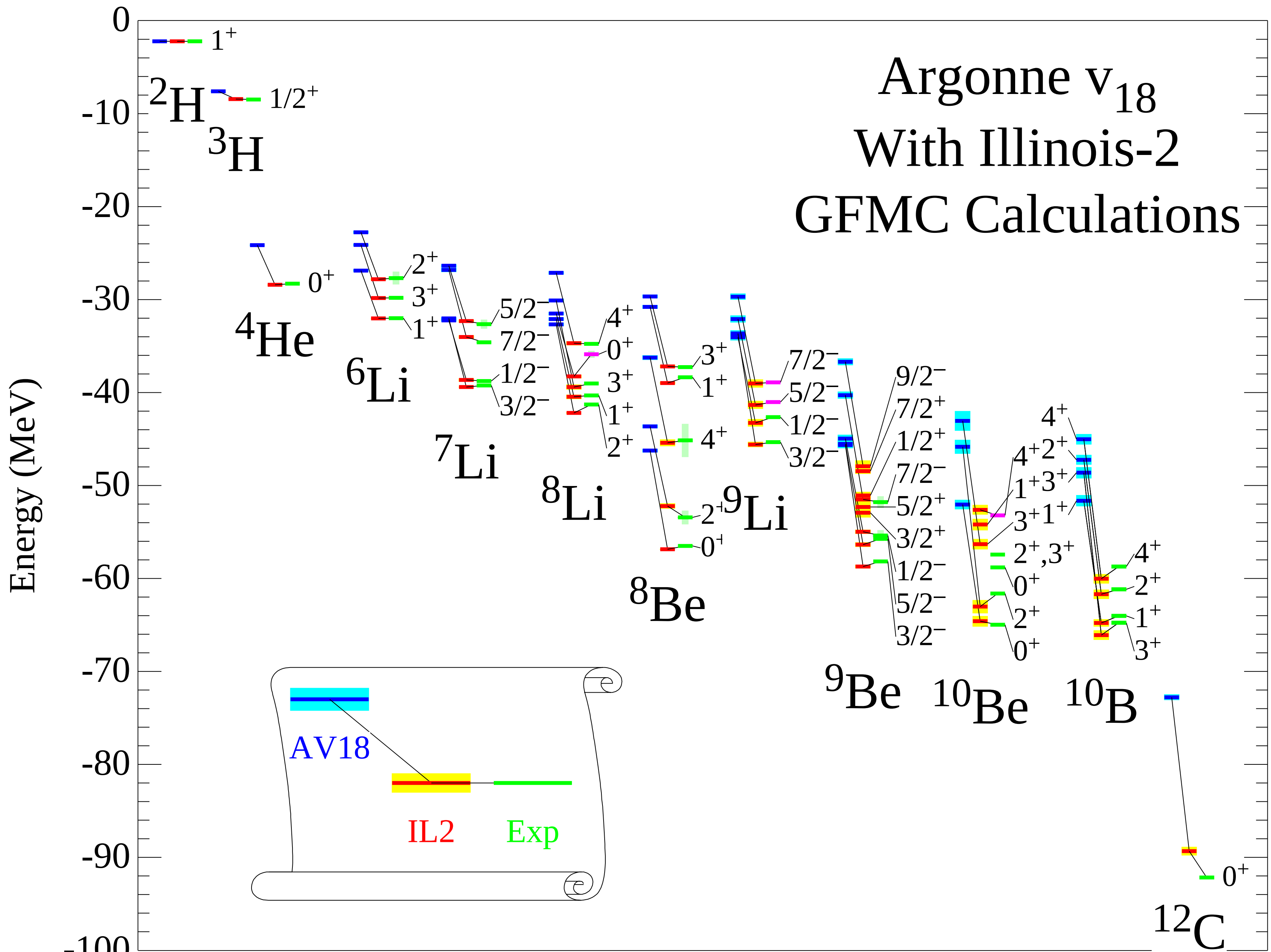

Argonne v18
With Illinois-2
GFMC Calculations
Energy (MeV)
0
-10
-20
-30
-40
-50
-60
-70
-80
-90
-100
2H
3H
4He
6Li
7Li
8Li
8Be
9Li
9Be
10Be
10B
12C
AV18
IL2
Exp

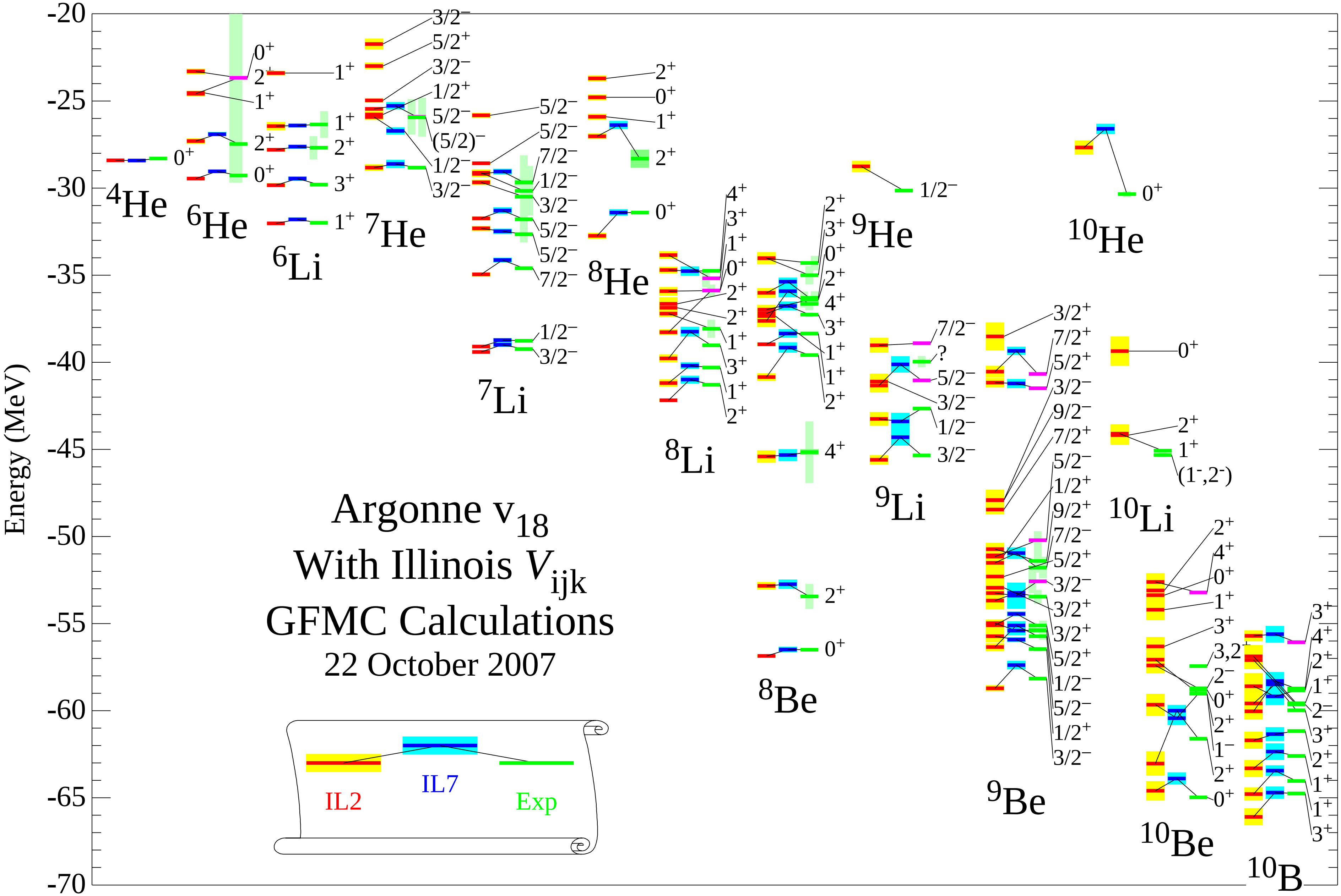

Energy (MeV)
-20
-25
-30
-35
-40
-45
-50
-55
-60
-65
-70
^{4}He
0^{+}
^{6}He
0^{+} 2^{+} 1^{+} 2^{+} 0^{+}
^{6}Li
1^{+} 1^{+} 2^{+} 3^{+} 1^{+}
^{7}He
3/2^{-} 5/2^{+} 3/2^{-} 1/2^{+} 5/2^{-} (5/2)$^{-}$ 1/2^{-} 3/2^{-}
^{7}Li
5/2^{-} 5/2^{-} 7/2^{-} 1/2^{-} 3/2^{-} 5/2^{-} 5/2^{-} 7/2^{-} 1/2^{-} 3/2^{-}
^{8}He
2^{+} 0^{+} 1^{+} 2^{+} 0^{+}
^{8}Li
4^{+} 3^{+} 1^{+} 0^{+} 2^{+} 2^{+} 1^{+} 3^{+} 1^{+} 2^{+}
^{8}Be
2^{+} 3^{+} 0^{+} 2^{+} 4^{+} 3^{+} 1^{+} 1^{+} 2^{+} 4^{+} 2^{+} 0^{+}
^{9}He
1/2^{-}
^{10}He
0^{+}
^{9}Li
7/2^{-} ? 5/2^{-} 3/2^{-} 1/2^{-} 3/2^{-}
^{9}Be
3/2^{+} 7/2^{+} 5/2^{+} 3/2^{-} 9/2^{-} 7/2^{+} 5/2^{-} 1/2^{+} 9/2^{+} 7/2^{-} 5/2^{+} 3/2^{-} 3/2^{+} 3/2^{+} 5/2^{+} 1/2^{-} 5/2^{-} 1/2^{+} 3/2^{-}
^{10}Li
0^{+} 2^{+} 1^{+} (1^{-},2^{-})
^{10}Be
2^{+} 4^{+} 0^{+} 1^{+} 3^{+} 3,2^{+} 2^{-} 0^{+} 2^{+} 1^{-} 2^{+} 0^{+}
^{10}B
3^{+} 4^{+} 2^{+} 1^{+} 2^{-} 3^{+} 2^{+} 1^{+} 1^{+} 3^{+}
Argonne v_{18}
With Illinois V_{ijk}
GFMC Calculations
22 October 2007
IL2
IL7
Exp

Nolen-Schiffer Anomaly

Extract isovector [CSB $\propto (\tau_i + \tau_j)_z$] & isotensor [CD $\propto T_{ij}$] energy components:

$$E_{A,T}(T_z) = \sum_{n \leq 2T} a_n(A,T)Q_n(T,T_z)$$

$Q_0 = 1\,;\, Q_1 = T_z\,;\, Q_2 = \frac{1}{2}(3T_z^2 - T^2)$

Strong Type III CSB (constrained $\pm 20\%$ by nn scattering length) fixes isovector terms.

Strong Type II CD (constrained by ${}^1\mathrm{S}_0$ pp and np scattering) overdoes isotensor; need P-wave NN scattering constraint?

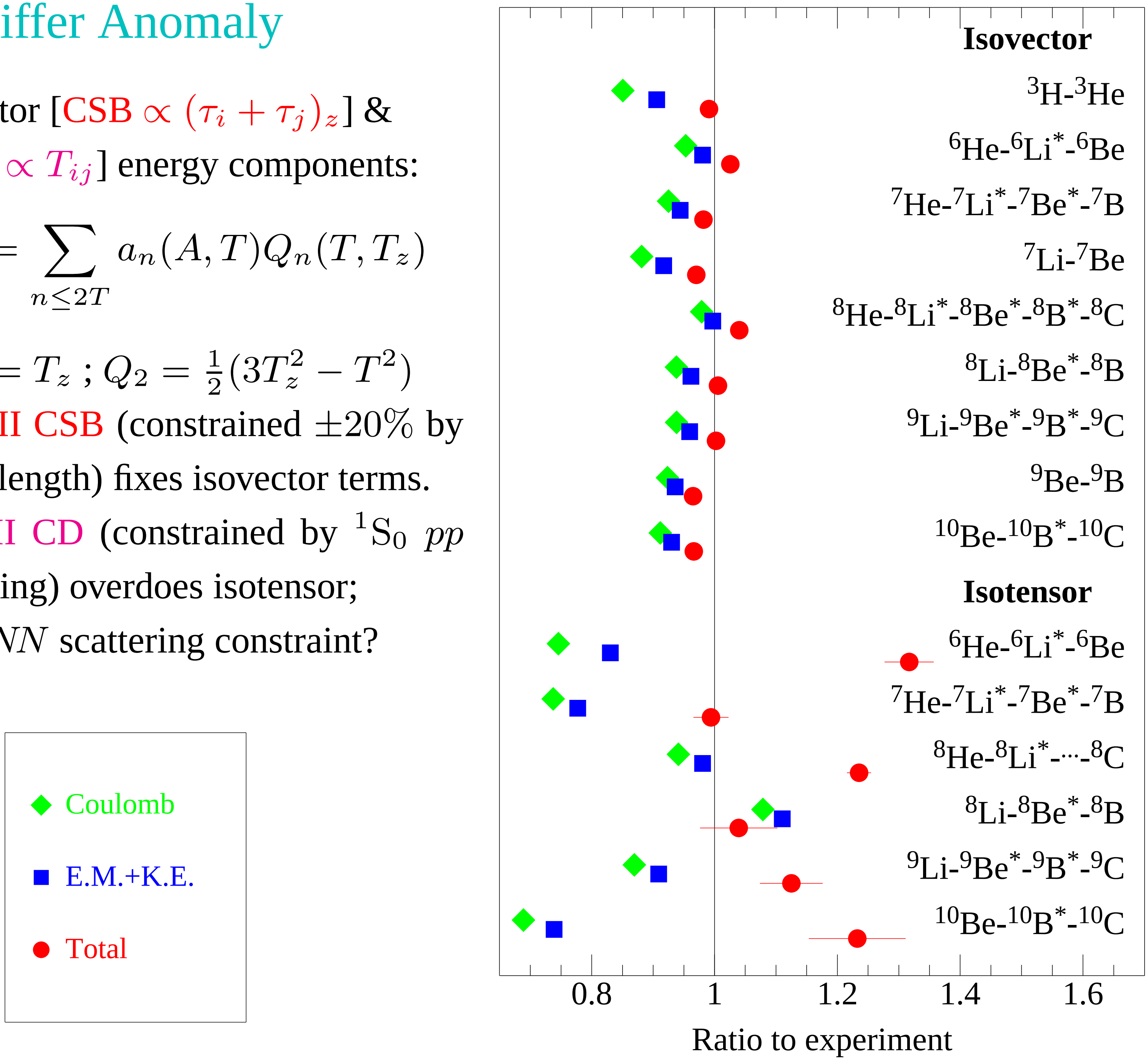

GFMC isovector and isoscalar energy coefficients for AV18+IL7 in keV

$a_n(A,T)$	K^{CSB}	$v_{C1}(pp)$	$v^{\gamma,R}$	v^{CSB}+v^{CD}	Total	Expt.
$a_1(3,\frac{1}{2})$	14	650(0)	28	65(0)	757(0)	764
$a_1(6,1)$	18	1118(2)	14	54(1)	1203(2)	1173
$a_1(7,\frac{1}{2})$	23	1446(3)	36	86(1)	1592(4)	1641
$a_1(7,\frac{3}{2})$	17	1270(3)	9	52(1)	1348(4)	1373
$a_1(8,1)$	23	1660(4)	19	78(1)	1780(5)	1770
$a_1(8,2)$	22	1624(4)	8	71(1)	1726(4)	1659
$a_1(9,\frac{1}{2})$	19	1709(6)	4	55(1)	1786(7)	1851
$a_1(9,\frac{3}{2})$	26	1974(6)	19	90(1)	2109(7)	2104
$a_1(10,1)$	25	2123(7)	18	55(1)	2250(8)	2329
$a_2(6,1)$		167(0)	19	109(8)	295(9)	224
$a_2(7,\frac{3}{2})$		129(0)	7	38(5)	174(5)	175
$a_2(8,1)$		137(1)	4	−10(8)	132(8)	145
$a_2(8,2)$		144(0)	6	39(3)	189(3)	127
$a_2(9,\frac{3}{2})$		153(1)	7	38(8)	198(9)	176
$a_2(10,1)$		166(1)	12	119(18)	297(19)	241

Isospin-mixing in ^{8}Be

Experimental energies of 2^+ states

E_a = 16.626(3) MeV Γ_a^α = 108.1(5) keV

E_b = 16.922(3) MeV Γ_b^α = 74.0(4) keV

Isospin mixing of 2^+;1 and 2^+;0*

states due to isovector interaction H_{01}:

$\Psi_a = \beta\Psi_0 + \gamma\Psi_1$; $\Psi_b = \gamma\Psi_0 - \beta\Psi_1$

decay through $T = 0$ component only

$\Gamma_a^\alpha/\Gamma_b^\alpha = \beta^2/\gamma^2 \Rightarrow \beta = 0.77$; $\gamma = 0.64$

$$E_{a,b} = \frac{H_{00} + H_{11}}{2} \pm \sqrt{\left(\frac{H_{00} - H_{11}}{2}\right)^2 + (H_{01})^2}$$

$H_{00} = 16.746(2)$ MeV

$H_{11} = 16.802(2)$ MeV

$H_{01} = -145(3)$ keV

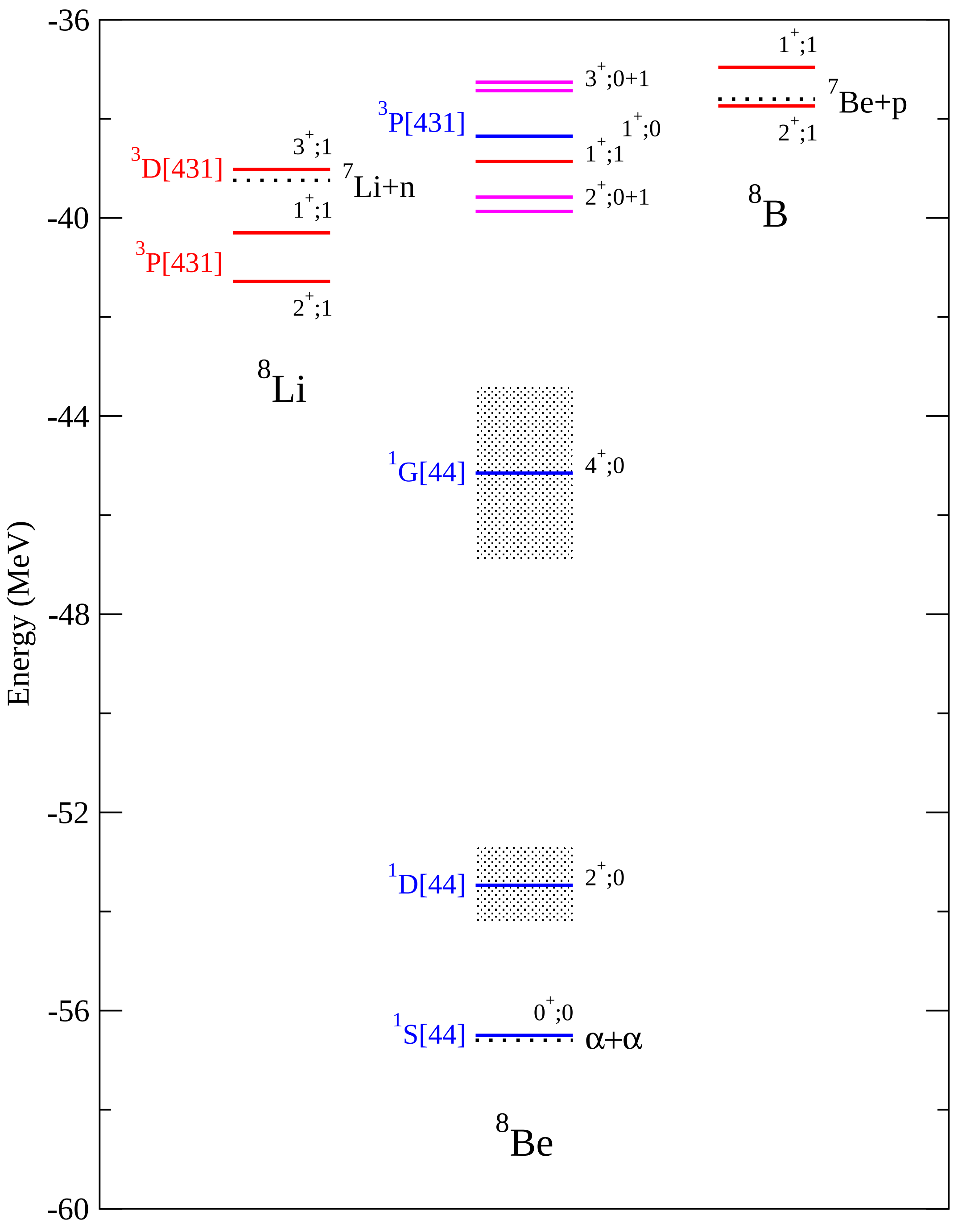

Isospin-mixing matrix elements in keV

		H_{01}	K^{CSB}	V^{CSB}	V_γ	(Coul)	(MM)
$2^+;1 \Leftrightarrow 2^+_2;0$	GFMC	$-115(3)$	$-3.1(2)$	$-21.3(6)$	$-90.3(26)$	$-78.3(25)$	$-12.0(2)$
	Barker	$-145(3)$				-67	
$1^+;1 \Leftrightarrow 1^+;0$	GFMC	$-102(4)$	$-2.9(2)$	$-18.2(6)$	$-80.3(30)$	$-79.5(30)$	$-0.8(2)$
	Barker	$-120(1)$				-54	
$3^+;1 \Leftrightarrow 3^+;0$	GFMC	$-90(3)$	$-2.5(2)$	$-14.8(6)$	$-73.1(21)$	$-60.9(21)$	$-12.2(2)$
	Barker	$-62(15)$				-32	
$2^+;1 \Leftrightarrow 2^+_1;0$	GFMC	$-6(2)$	$-0.4(2)$	$-1.3(4)$	$-4.4(12)$		

Barker, Nucl.Phys. **83**, 418 (1966)

Coulomb terms are about half of H_{01}, but magnetic moment and strong Type III CSB are relatively more important than in Nolen-Schiffer anomaly; still missing $\approx 20\%$ of strength.

Strong Type IV CSB will also contribute (probably best nuclear structure place to look):

$$\begin{aligned} V_{IV}^{CSB} &= (\tau_i - \tau_j)_z (\sigma_i - \sigma_j) \cdot \mathbf{L}\, v(r) \\ &+ (\tau_i \times \tau_j)_z (\sigma_i \times \sigma_j) \cdot \mathbf{L}\, w(r) \end{aligned}$$

Preliminary result: $v^\gamma \propto \mu_n \sim -2$ keV & $w^\pi \propto (M_n - M_p) \sim -2$ keV.

Single-nucleon densities

$$\rho_{p,n}(r) = \sum_i \langle \Psi | \delta(r - r_i) \frac{1 \pm \tau_i}{2} | \Psi \rangle$$

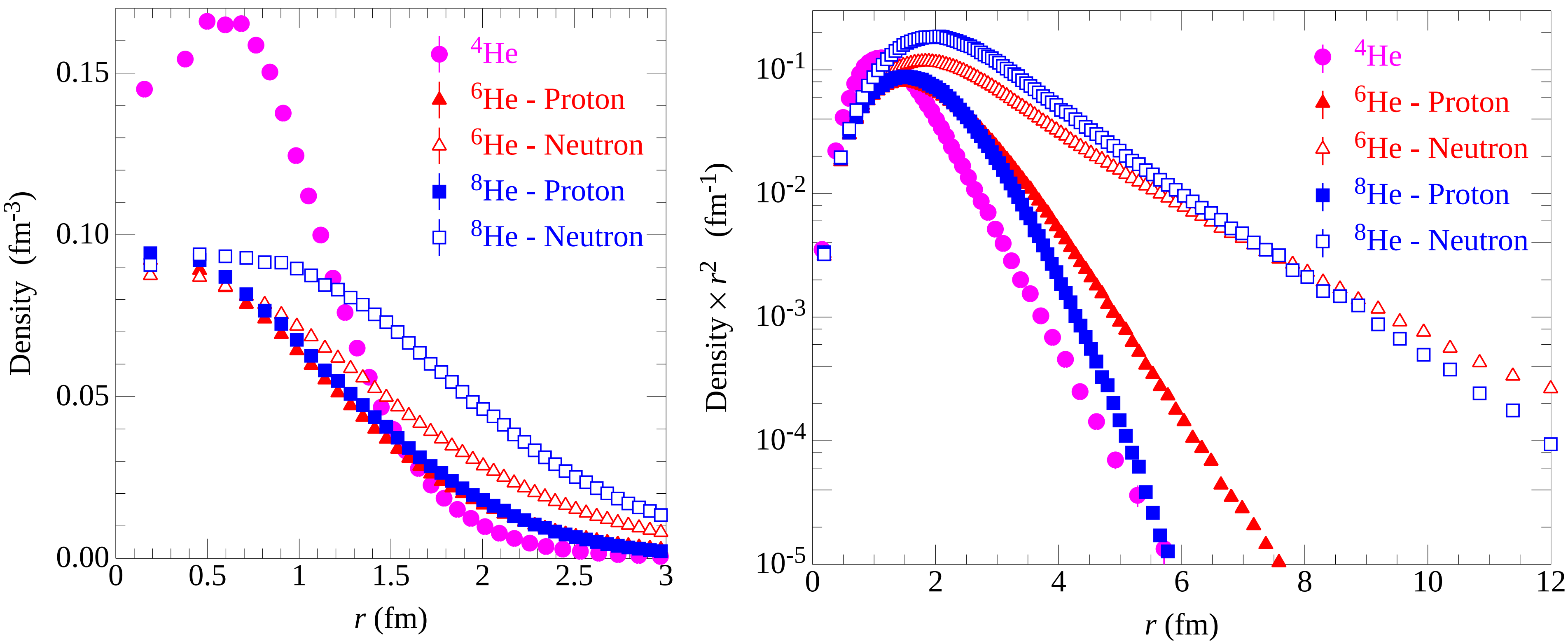

RMS radii

	r_n	r_p	r_c	Expt
^{4}He	1.45(1)	1.45(1)	1.67(1)	1.681(4)*
^{6}He	2.86(6)	1.92(4)	2.06(4)	2.072(9)†
^{8}He	2.79(3)	1.82(2)	1.94(2)	1.961(16)‡

*Sick, PRC **77**, 041302(R) (2008)

†Wang, *et al.*, PRL **93**, 142501 (2004)

‡Mueller, *et al.*, PRL **99**, 252501 (2007)

Two-nucleon densities

$$\rho_{pp}(r) = \sum_{i<j} \langle \Psi | \delta(r - |\mathbf{r}_i - \mathbf{r}_j|) \frac{1+\tau_i}{2} \frac{1+\tau_j}{2} | \Psi \rangle$$

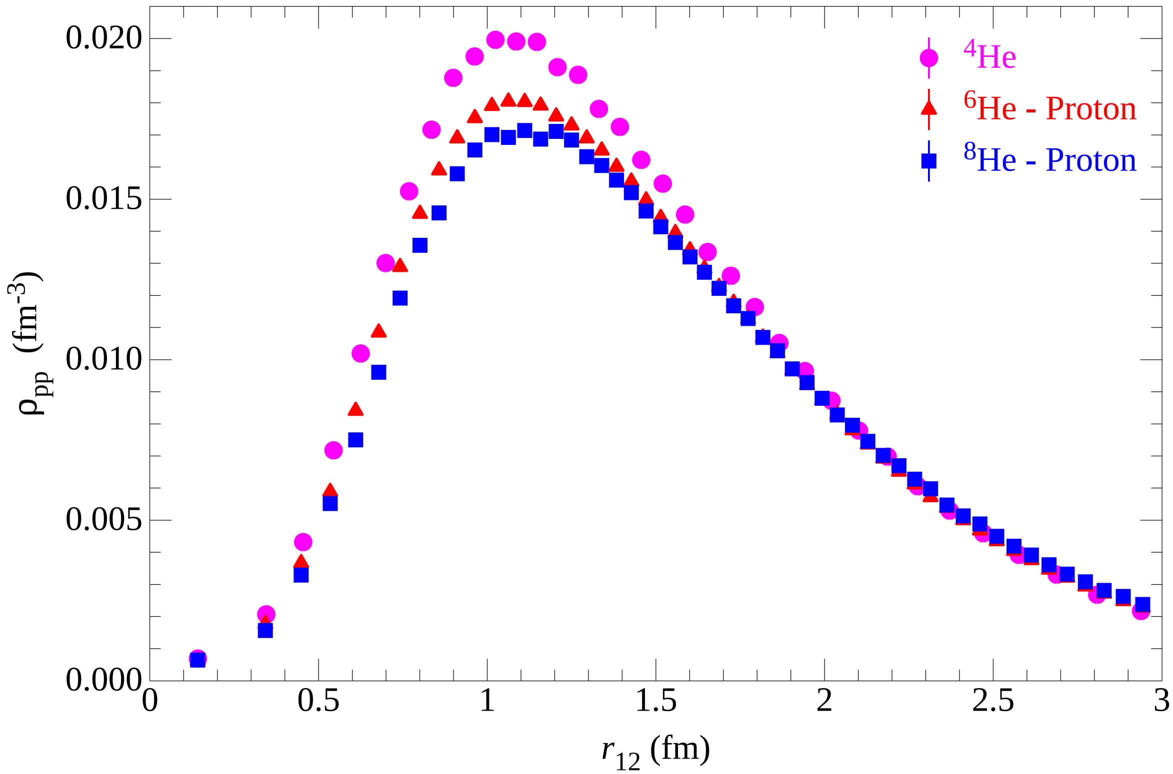

RMS radii

	r_{pp}	r_{np}	r_{nn}
^{4}He	2.41	2.35	2.41
^{6}He	2.51	3.69	4.40
^{8}He	2.52	3.58	4.37

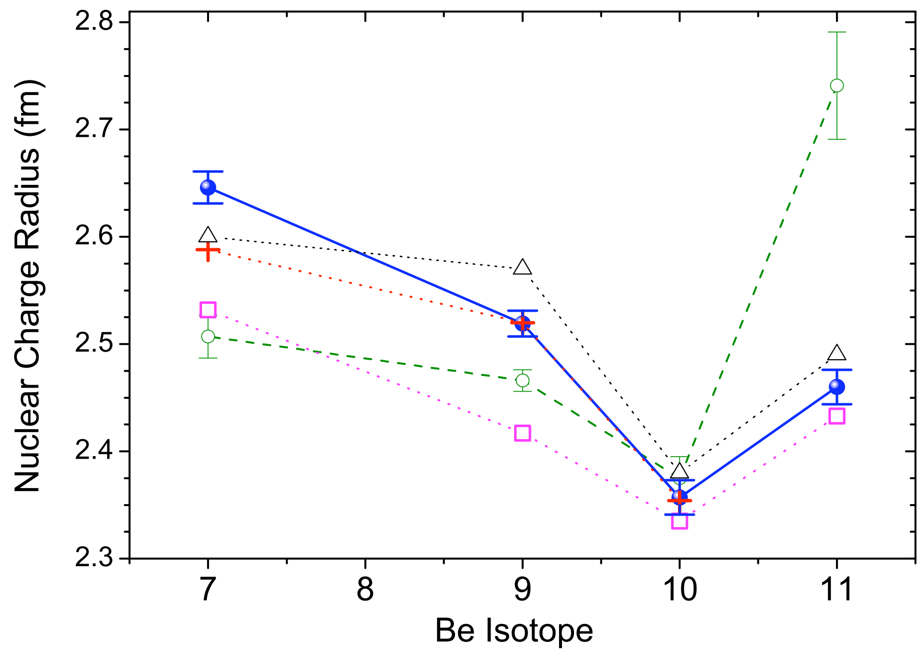

FIG. 3: (Color online) Experimental charge radii of beryllium isotopes from isotope shift measurements (●) compared with values from interaction cross section measurements (○) and theoretical predictions: Greens-Function Monte-Carlo calculations (+) [20, 21], Fermionic Molecular Dynamics (△) [22], *ab-initio* No-Core Shell Model (□) [12, 23, 24].

Nörtershäuser, *et al.*, arXiv:0809.2607

Nuclear Electromagnetic Currents

Marcucci *et al.* (2005)

$$\mathbf{j} = \mathbf{j}^{(1)}$$
$$+\, \mathbf{j}^{(2)}(\mathrm{v}) +$$

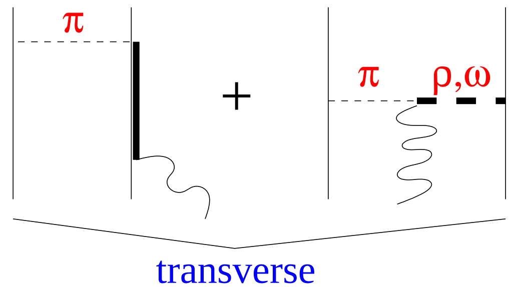

$$+\, \mathbf{j}^{(3)}(\mathrm{V}^{2\pi})$$

- Gauge invariant:

$$\mathbf{q} \cdot \left[\mathbf{j}^{(1)} + \mathbf{j}^{(2)}(v) + \mathbf{j}^{(3)}(V^{2\pi})\right] = \left[T + v + V^{2\pi}\,,\ \rho\right]$$

ρ is the nuclear charge operator

Magnetic Moments

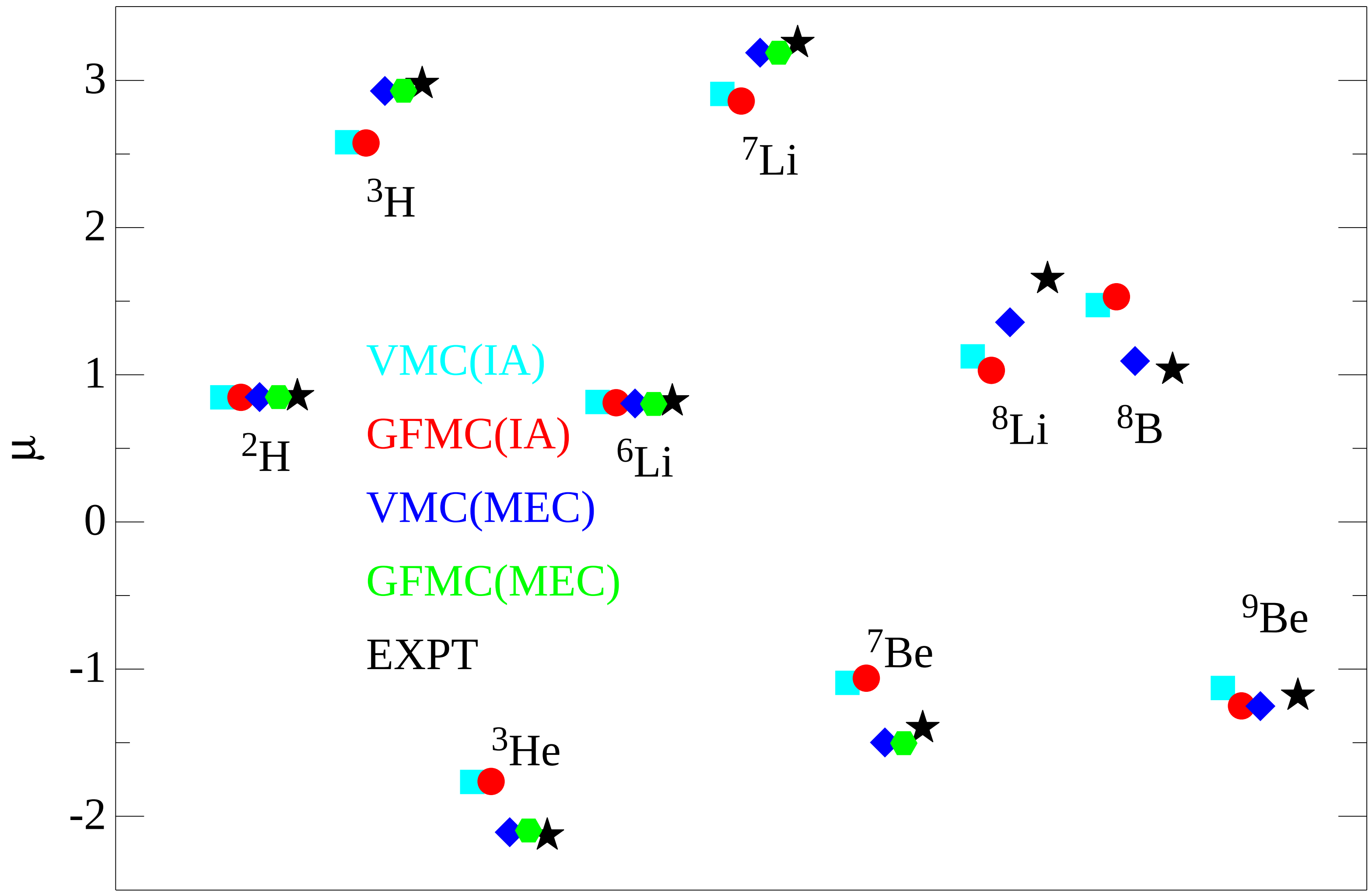

Marcucci, Pervin, *et al.* (arXiv:0810.0547)

$M1$, $E2$, F, GT transitions

$$E2 = e\sum_k \frac{1}{2}\left[r_k^2 Y_2(\hat{r}_k)\right](1+\tau_{kz})$$

$$M1 = \mu_N \sum_k [(L_k + g_p S_k)(1+\tau_{kz})/2 + g_n S_k \ (1-\tau_{kz})/2]$$

$$\mathrm{F} = \sum_k \tau_{k\pm} \ ; \ \mathrm{GT} = \sum_k \sigma_k \tau_{k\pm}$$

Pervin, Pieper & Wiringa, PRC **76**, 064319 (2007)

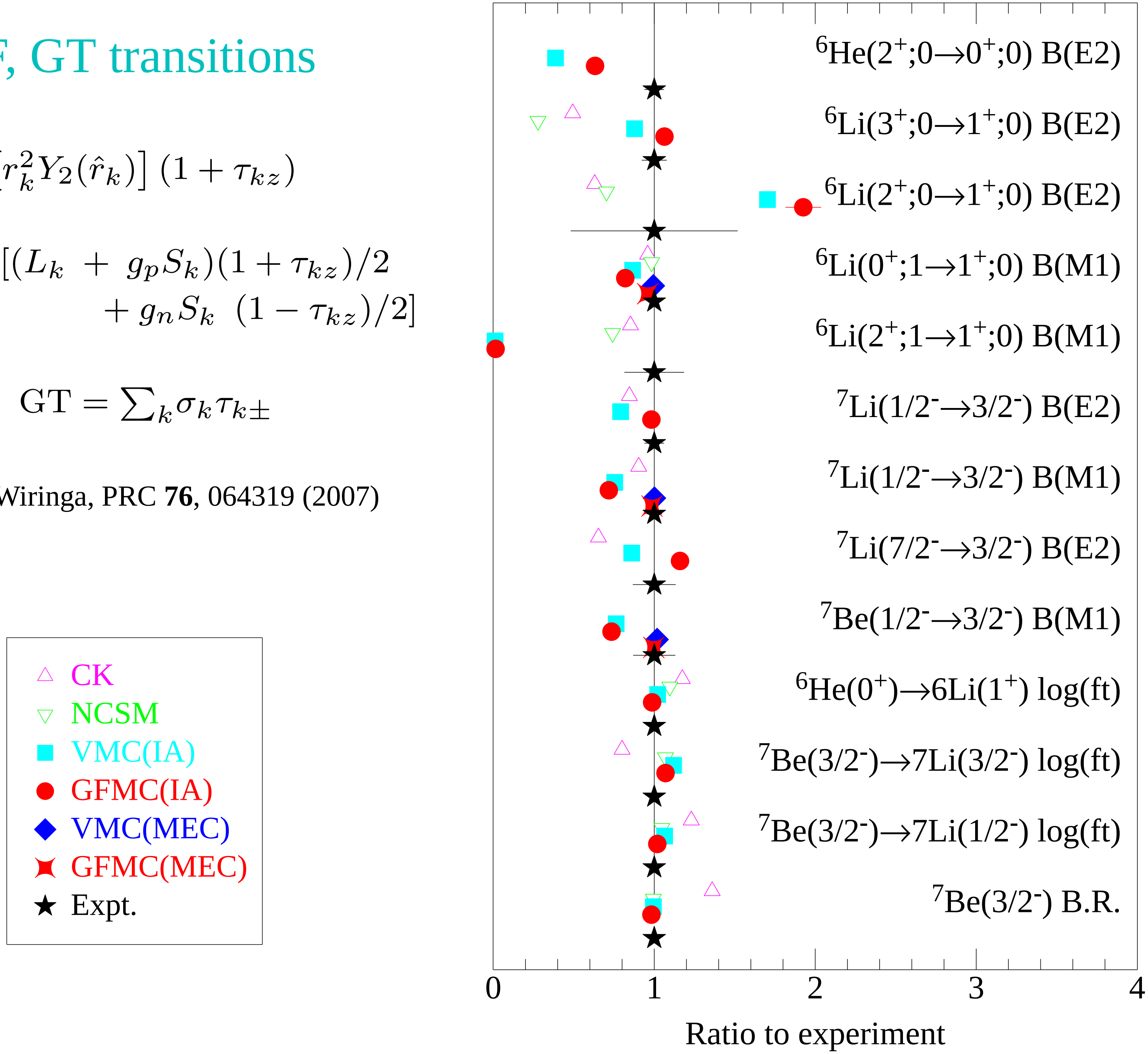

$^{10}\mathrm{Be}(2^+)$ levels

$^{10}\mathrm{Be}(2^+)$ levels at 3.37 and 5.96 MeV have same $^1\mathrm{D}_2[442]$ spatial symmetry.
Calculations give large but opposite sign quadrupole moments $Q \approx \pm 50$ mb.
Level ordering depends on H.

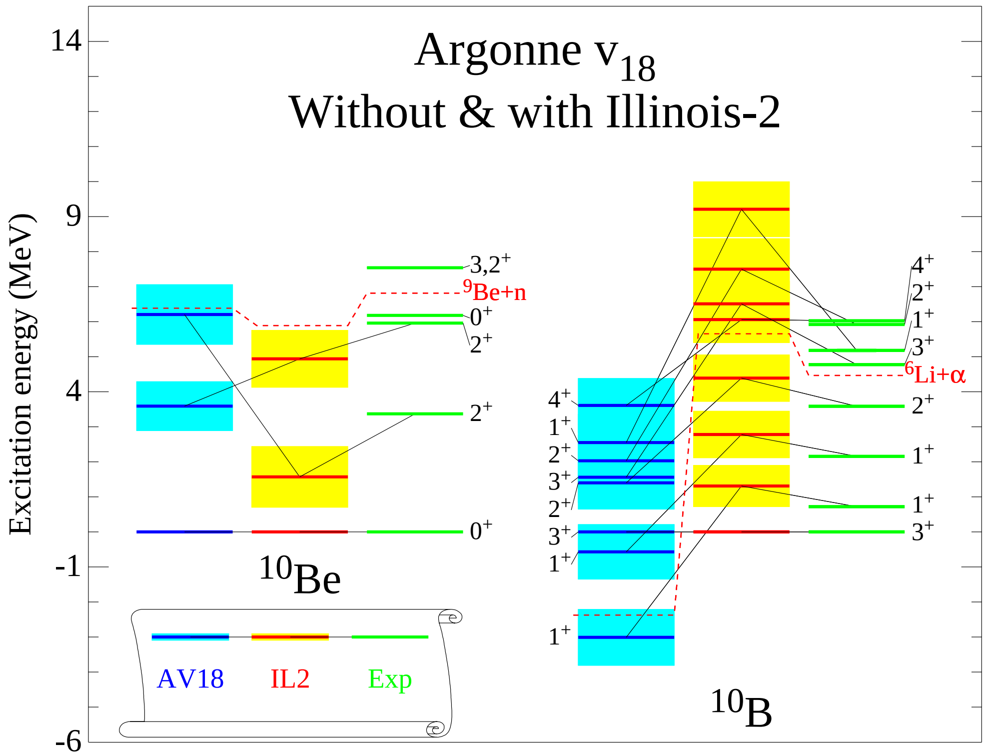

GFMC calculations of B($E2\downarrow$) give:
$^{10}\mathrm{Be}(2^+; Q<0) = 7.9(3) e^2\mathrm{fm}^4$
$^{10}\mathrm{Be}(2^+; Q>0) = 2.1(3) e^2\mathrm{fm}^4$
compared to experimental compendium
$^{10}\mathrm{Be}(2^+_1; 3.37) = 10.5(1.0) e^2\mathrm{fm}^4$

McCutchan & Lister doing ATLAS experiment to study transitions among these states – preliminary result:
$^{10}\mathrm{Be}(2^+_1; 3.37):\ \ 7.9(1.0) e^2\mathrm{fm}^4$
suggesting first 2^+ state has $Q<0$

Calculations for $2^+_2 \rightarrow 2^+_1$ give:
B($E2\downarrow$) $= 6.9(1.0) e^2\mathrm{fm}^4$ (GFMC)
B($M1\downarrow$) very small (VMC)
Previous experiment found mostly $M1$

GFMC for scattering states

GFMC treats nuclei as particle-stable system – should be good for energies of narrow resonances

Need better treatment for locations and widths of wide states and for capture reactions

Method

- Pick a logarithmic derivative, χ, at some large boundary radius ($R_B \approx 9$ fm)
- GFMC propagation, using method of images to preserve χ at R, finds $E(R_B, \chi)$
- Phase shift, $\delta(E)$, is function of R_B, χ, E
- Repeat for a number of χ until $\delta(E)$ is mapped out

Example for $^5\mathrm{He}(\frac{1}{2}^-)$

- "Bound-state" boundary condition does not give stable energy; Decaying to n+^{4}He threshold
- Scattering boundary condition produces stable energy.

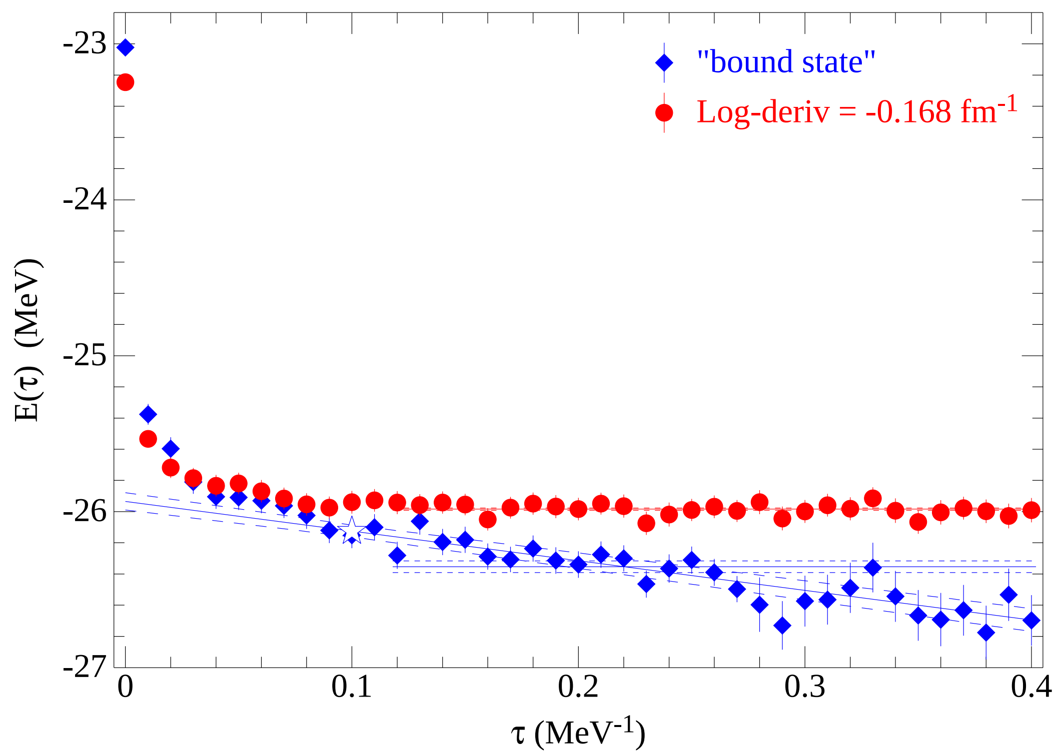

GFMC for ^{5}He as n+^{4}He Scattering States

Black curves: Hale phase shifts from R-matrix analysis up to $J = \frac{9}{2}$ of data

AV18 with no V_{ijk} underbinds ^{5}He($3/2^-$) & overbinds ^{5}He($1/2^-$)

AV18+UIX improves ^{5}He($1/2^-$) but still too small spin-orbit splitting

AV18+IL2 reproduces locations and widths of both P-wave resonances

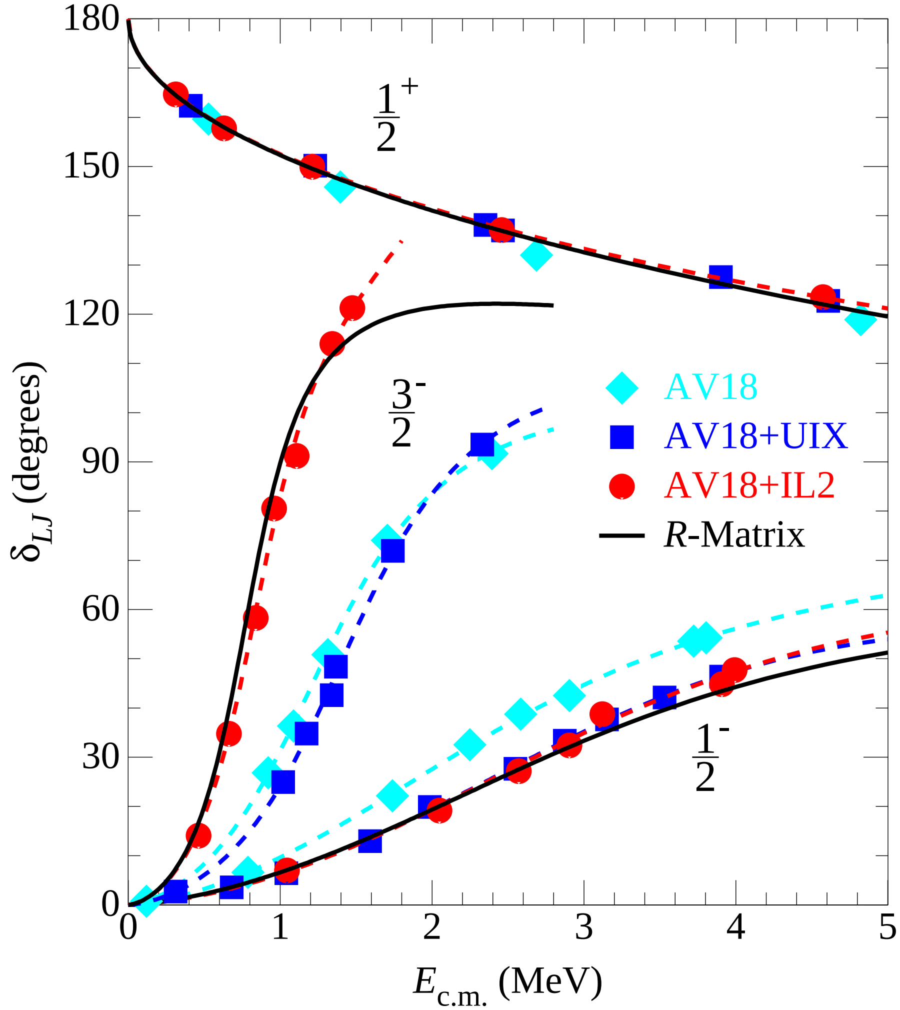

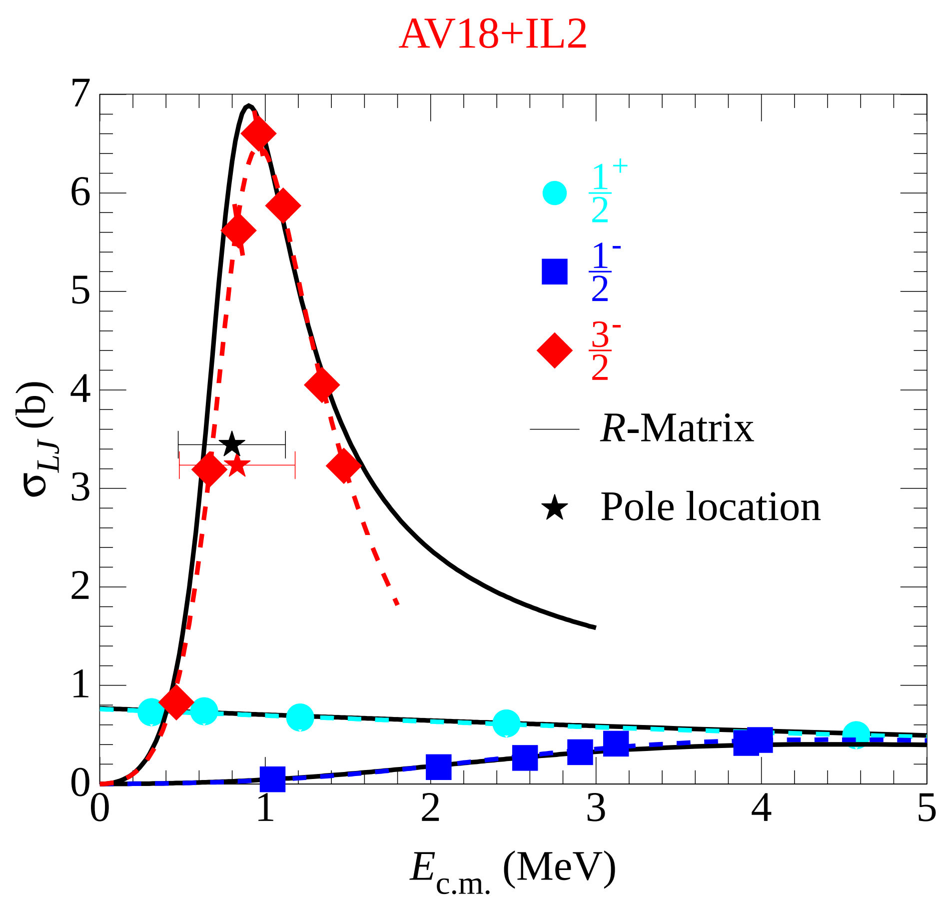

Nollett, *et al.*, PRL **99**, 022502 (2007)

RADIATIVE CAPTURE REACTIONS

$$\sigma(E_{cm}) = \frac{8\pi}{3}\frac{\alpha}{v_{\rm rel}}\frac{q}{1+q/m_{\rm Li}}\sum_{LSJ\ell}\left[\left|E_\ell^{LSJ}(q)\right|^2 + \left|M_\ell^{LSJ}(q)\right|^2\right]$$

^{3}H$(\alpha,\gamma)^7$Li ^{3}He$(\alpha,\gamma)^7$Be

Sources of ^{7}Li in big bang

^{7}Be key to solar ν_e production

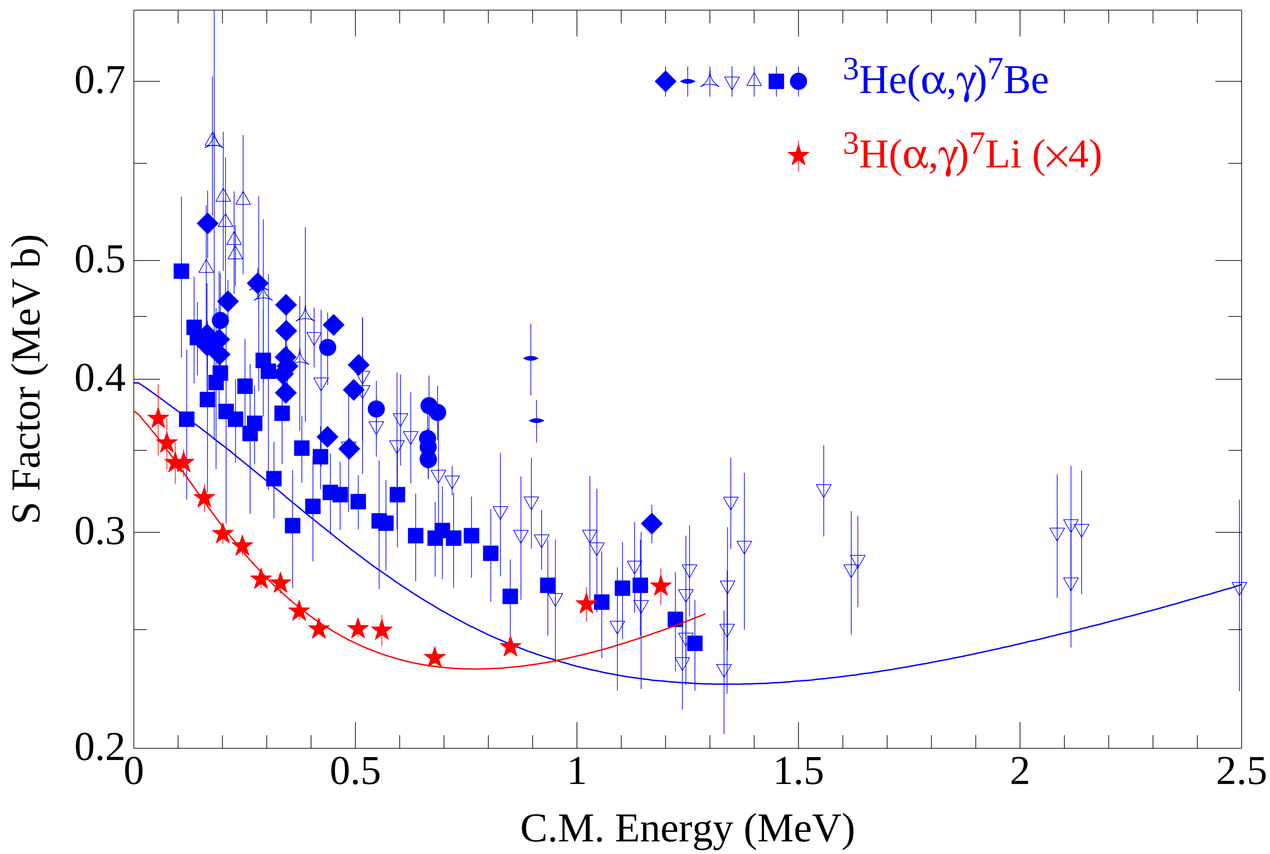

Nollett, PRC **63**, 054002 (2001)

Single-nucleon momentum distributions

$$\rho_{\sigma\tau}(k) = \int d\mathbf{r}'_1\, d\mathbf{r}_1\, d\mathbf{r}_2\, \cdots d\mathbf{r}_A\, \psi^\dagger_{JM_J}(\mathbf{r}'_1, \mathbf{r}_2, \ldots, \mathbf{r}_A)\, e^{-i\mathbf{k}\cdot(\mathbf{r}_1-\mathbf{r}'_1)}\, P_{\sigma\tau}(1)\, \psi_{JM_J}(\mathbf{r}_1, \mathbf{r}_2, \ldots, \mathbf{r}_A)$$

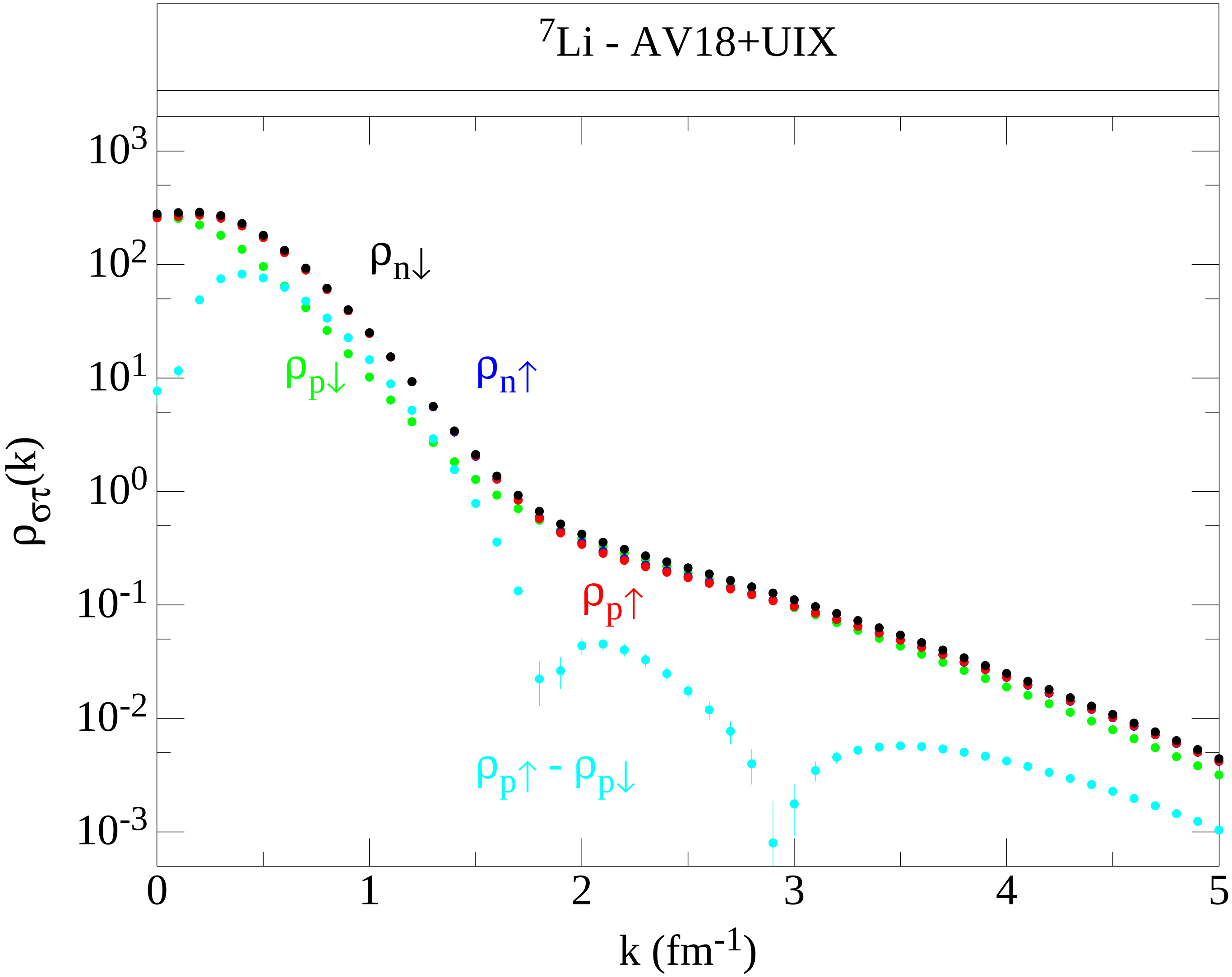

TWO-NUCLEON & CLUSTER-CLUSTER DISTRIBUTIONS

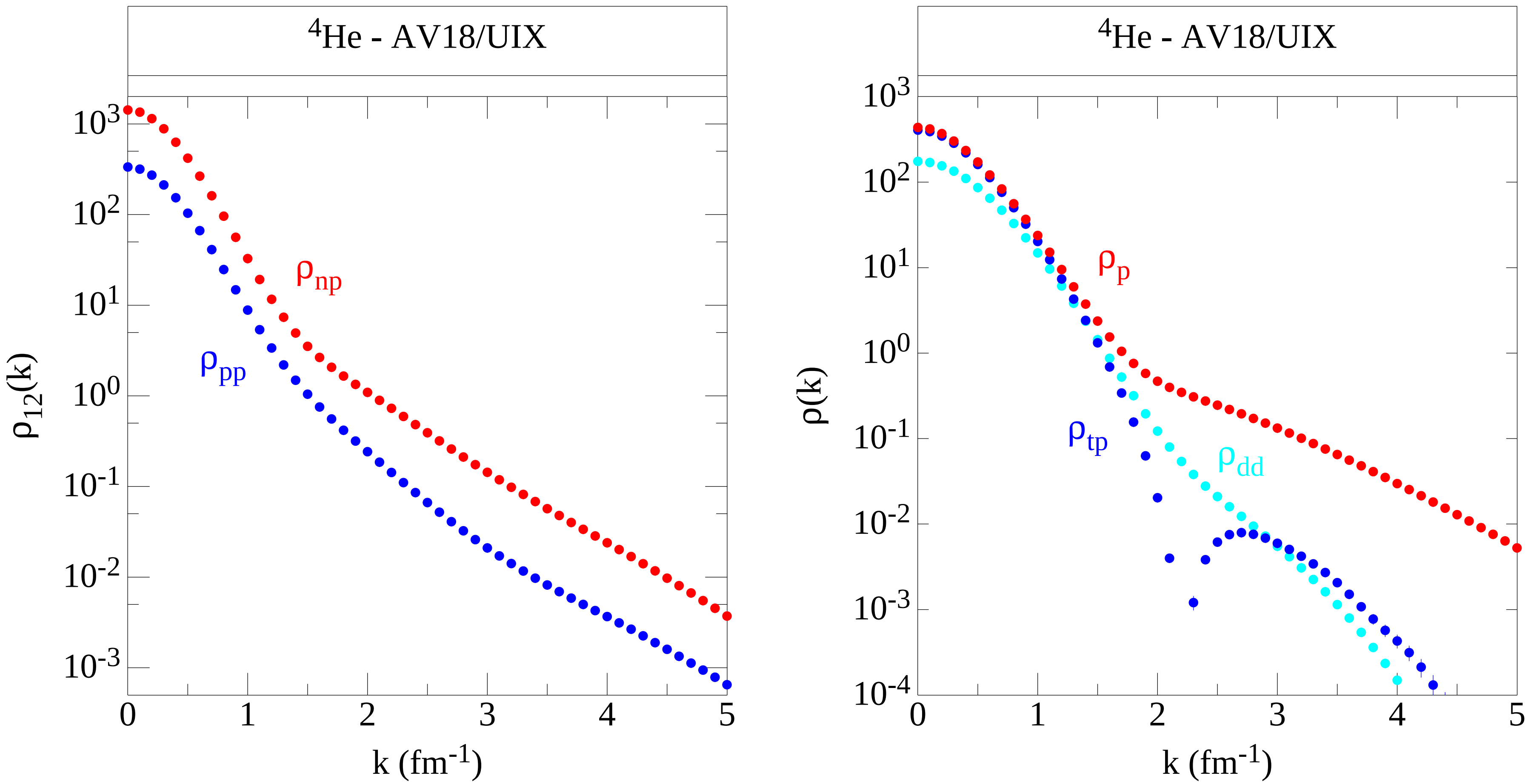

Two-nucleon Knockout – $A(e, e'pN)$

JLAB experiment for ^{12}C$(e, e'pN)$ measured back-to-back pp and np pairs

Pairs with $q_{\rm rel}$ = 2–3 fm^{-1} show np/pp ratio ≈ 10–20   Subedi *et al.*, Science **320**, 1476 (2008)

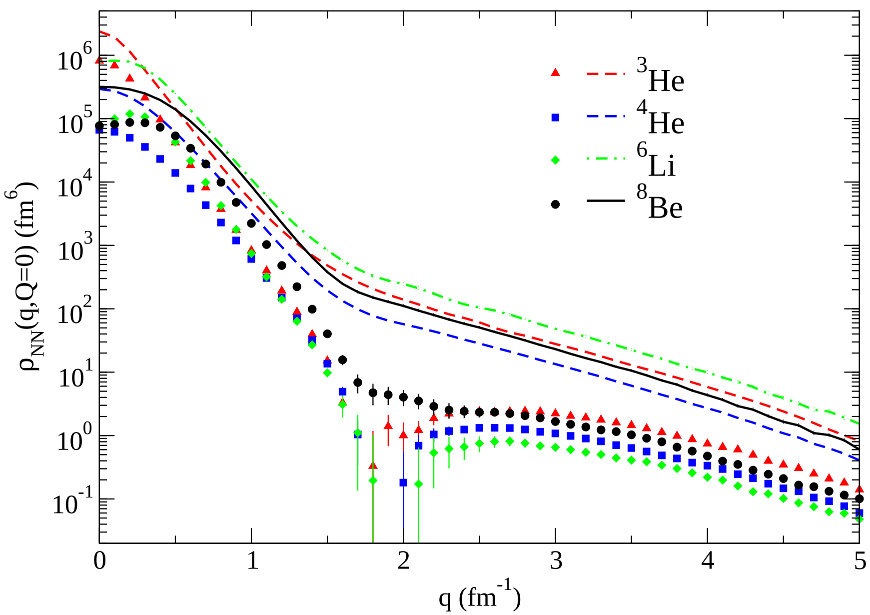

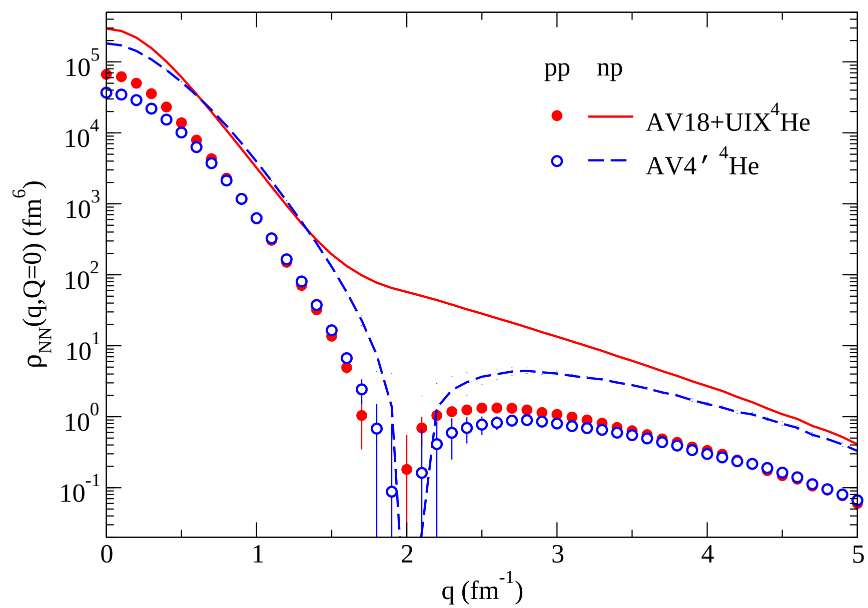

VMC calculations for pairs with $Q_{\rm tot}$ = 0 show this effect in A=3–8 nuclei

Effect disappears when tensor correlations are turned off

Shows importance of tensor correlations to > 3 fm^{-1}

Schiavilla, Wiringa, Pieper & Carlson, PRL **98**, 132501 (2007)

For $Q_{\rm tot} > 0$ $(Q \parallel q)$, the minimum in pp distribution fills in:

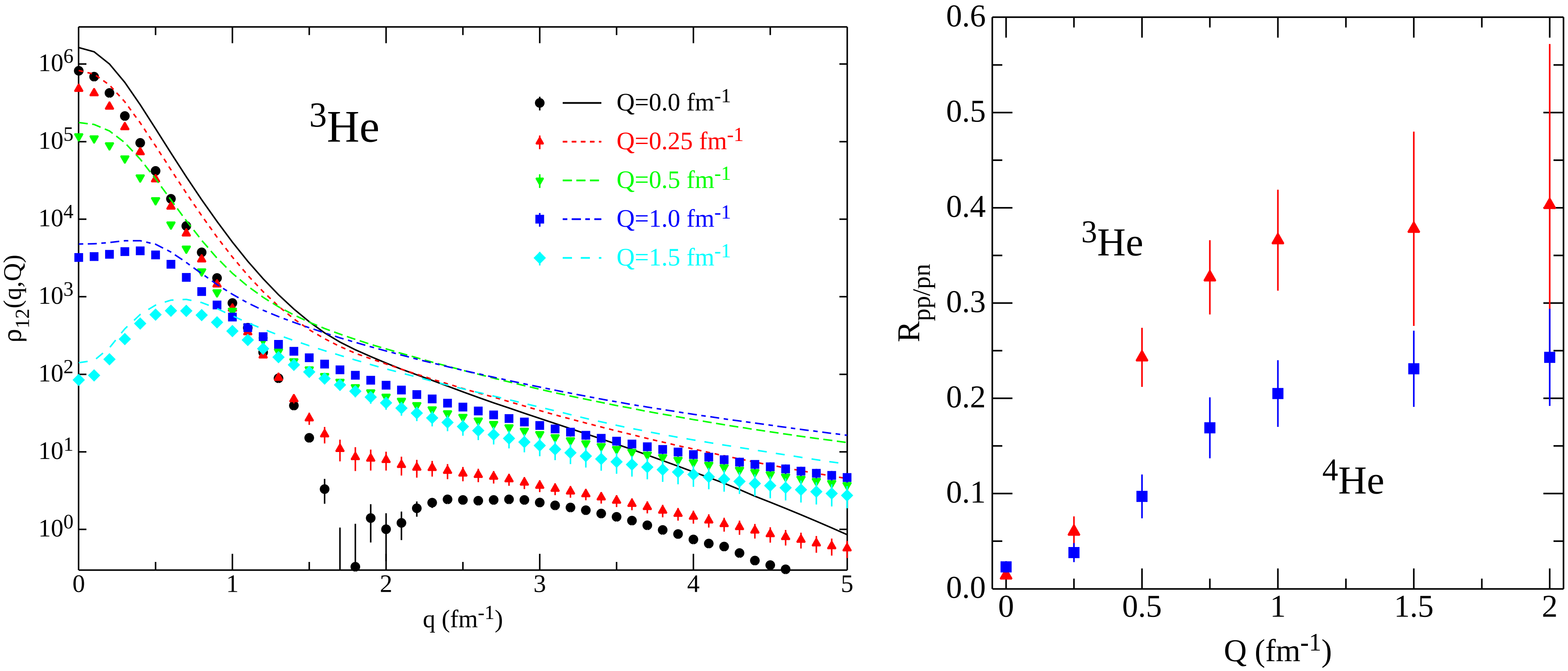

For $q_{\rm rel}$ integrated over 300–500 MeV/c, the ratio of pp to pn pairs $R_{pp/pn}$ compares well with preliminary analysis of CLAS data for ^{3}He$(e, e'pp)n$

Wiringa, Schiavilla, Pieper & Carlson, PRC **78**, 021001 (2008)

CONCLUSIONS

ADVANTAGES/LIMITATIONS

- No basis required - very general trial functions with proper asymptotic structure can be used
- limited to configuration-space local potentials
- calculation requirements grow exponentially with A
- Most accurate method for $5 \leq A \leq 12$

BENCHMARKS

- neutron drops ${}^{8-14}n$ for UNEDF
- ^{12}C ground state energy, 2^+ excited state, form factors
- ^{12}C(0_2^+) triple-alpha resonance

EXPERIMENTS

- charge radii (both absolute and relative along isotope chains)
- B($M1$), B($E2$), B(GT), etc. for $6 \leq A \leq 12$ with modern methods